Research Paper
Computational Methods for Differential Equations
http://cmde.tabrizu.ac.ir
Vol. *, No. *, *, pp. 1-20
DOI:10.22034/cmde.2026.67629.3230

Numerical solution of nonlinear fractional delay differential equations using fractional Jacobi functions and Picard iteration

Soheyla Ansari and Mohammad Hossein Akrami*
Department of Mathematical Sciences, Yazd University, Yazd, Iran.

Abstract

This paper presents a novel numerical method for solving nonlinear fractional delay differential equations. Our approach uses fractional Jacobi functions in conjunction with a straightforward Picard iteration scheme to construct numerical solutions. Unlike some existing techniques, the proposed method is computationally efficient and avoids complex calculations. The use of orthogonal functions within the Picard iterations provides accurate approximations. Also, a convergence analysis demonstrates the method's high accuracy. We demonstrate the method's applicability and effectiveness by solving several challenging fractional delay differential equations, including the fractional pantograph equation and the fractional Hutchinson model. The results confirm that our method performs better than other numerical methods.

Keywords. Fractional Jacobi functions; Picard iterations method; Fractional pantograph equation; Fractional Hutchinson model.
2010 Mathematics Subject Classification. 65L05, 34K06, 34K28.

1. Introduction

In the mathematical modeling of physical processes, it is commonly assumed that a system's behavior solely relies on its current state. This assumption is valid for a wide range of dynamic systems. However, there are circumstances where this assumption fails, leading to potentially suboptimal performance when classical models are used for system analysis and design. In such cases, it is more appropriate to account for the influence of the system's previous states on its behavior. These systems are referred to as time-delay systems. Over recent decades, delay systems have attracted considerable interest from researchers. Time-delay systems are significant in various fields, such as engineering, physics, chemistry, disease modeling [44], and traffic flow modeling [40]. The theory of delay differential equations was introduced by Myshkis in 1949 [28]. Additionally, notable contributions in this field have been made by El'sgol'c and Norkin [29], Krasovski, Bellman and Cooke [11], and Hale [16].

Fractional delay differential equations (FDDEs) arise in different scientific and engineering disciplines, leading to a surge of research interest in developing effective numerical solution methods. These equations model phenomena in areas such as amorphous semiconductors, fractional random walks, fluid dynamics, probability and statistics, electrical networks, signal processing, and rheology. For a comprehensive overview of these applications, we direct the reader to reference [38]. Numerous effective numerical techniques have been developed for solving FDDEs. These include wavelet-based methods such as the Genocchi wavelet method [13], Haar wavelet collocation technique (HWCT) [3], a method by using fractional-order hybrid Bessel functions (FHBFs) [14], a Haar wavelet operational matrix method [21], a novel shifted Jacobi operational matrix method [22], higher order numerical methods [23], an operational matrix developed using Bernoulli wavelets [34], Fibonacci wavelets [37], fractional-order Fibonacci-hybrid functions method (FFHFM) [38], a robust method based on novel-operational matrices [42], modified an Adams-type method [30], the fractional generalized adams method [45], wavelet Galerkin [15], reproducing kernel [35], fitted mesh spline [36], piecewise Picard iteration method [9]. Furthermore, for optimal control problems, cubic B-spline [24] and hybrid

Received: 01 June 2025; Accepted: 07 July 2026.
∗ Corresponding author. Email: akrami@yazd.ac.ir.

block-pulse multiwavelet [27] methods have been proposed. Moreover, the stability and qualitative behavior of FDDEs and related systems have been investigated by several authors [7, 26].

The field of fractional calculus offers a variety of fractional operators, each with specific advantages and disadvantages. These include the Grünwald-Letnikov, Atangana-Baleanu, Caputo-Fabrizio, Riemann-Liouville, Katugampola, Caputo, Atangana-Gomez, ψ-Hilfer, and Hadamard operators [1, 17, 19, 20, 32, 33]. The Caputo fractional derivative is particularly well-suited for solving fractional differential equations. Its key strength lies in its handling of initial conditions involving integer order derivatives. This allows a more intuitive and physically meaningful approach to modeling systems with memory effects and complex dynamics, especially those exhibiting power-law memory kernels. The Caputo derivative's simpler physical interpretation, compared to other fractional derivatives, further contributes to its popularity in scientific applications [31].

The Picard iterative method is a common technique for solving fractional differential equations (FDEs). This method constructs a sequence of functions that iteratively converge to the exact solution. Each iteration refines the previous approximation, generating a sequence that progressively approaches the true solution. This successive approximation approach provides a powerful numerical tool for solving FDEs [5, 6, 9, 43]. A key challenge in implementing the Picard iteration method for fractional differential equations (FDEs) is evaluating the fractional integral at each step. To address this, inspired by Tafakkori-Bafghi et al. [41] and Zhou et al. [46], we utilize Jacobi polynomials (or functions) to simplify the integral computation. In this paper, we develop a novel method for efficiently solving FDEs with processing delays. This new approach provides a robust numerical solution for such systems. Iterative numerical techniques of this kind have demonstrated their value in classical numerical analysis, offering effective solutions for a wide range of differential equations across various applications.

This paper is structured as follows: Section 2, presents an overview of the essential concepts in fractional calculus, including discussions of orthogonal Jacobi polynomials and fractional Jacobi functions. Section 3, provides a comprehensive overview of the authors' main approach, including detailed mathematical explanations of the methodology used. Section 4, the focus shifts to a detailed examination of the convergence properties of the method presented in previous section. Section 5, includes several numerical examples that demonstrate the practical application and effectiveness of the proposed approach. The paper concludes with a final section summarizing the key findings.

2. Preliminaries

In this section, we begin by reviewing some key properties of fractional calculus theory, followed by an exploration of the properties of Jacobi polynomials, as discussed in references [4, 5, 8, 25].

2.1. The fractional derivative and integral.

The two most widely used definitions of fractional derivatives and integrals are the Riemann–Liouville and Caputo formulations, both of which have been developed more recently.

Definition 2.1. [25] The fractional integral operator of order $q > 0$, in sense of the Riemann–Liouville applied to a function $u(\xi)$, is defined as:

$$\mathcal{I}_0^q u(\xi) = \frac{1}{\Gamma(q)} \int_0^\xi (\xi - s)^{q-1} u(s) ds, \ 0 < \xi < L, \tag{2.1}$$

$$\mathcal{I}_0^0 u(\xi) = u(\xi), \tag{2.2}$$

where

$$\Gamma(q) = \int_0^\infty \xi^{q-1} \exp(-\xi) d\xi,$$

is the well-known gamma function.

The integral operator $\mathcal{I}^q$ defined in (2.1) has the following properties [25]:

$$\mathcal{I}_0^q \xi^k = \frac{\Gamma(q+1)}{\Gamma(q+1+k)} \xi^{q+k}, \tag{2.3}$$

$$\mathcal{I}_0^q \mathcal{I}_0^p u(\xi) = \mathcal{I}_0^{q+p} u(\xi) = \mathcal{I}_0^p \mathcal{I}_0^q u(\xi), \tag{2.4}$$

where $p, q \geq 0$ and $k \geq -1$. Similar to the case of integer-order integration, the Riemann–Liouville fractional integral operator is a linear operation:

$$\mathcal{I}_0^q(u(\xi) + v(\xi)) = \mathcal{I}_0^q u(\xi) + \mathcal{I}_0^q v(\xi),$$
$$\mathcal{I}_0^q(cu(\xi)) = c\mathcal{I}_0^q u(\xi),$$

where c is a scalar constant and $u(\xi)$ and $v(\xi)$ are arbitrary functions.

Definition 2.2. [25], The Caputo fractional derivative of order q is defined by the following expression:

$${}^c\mathcal{D}^q u(\xi) = \mathcal{I}_0^{n-q} u^{(n)}(\xi) = \frac{1}{\Gamma(n-q)} \int_0^\xi (\xi - s)^{n-q-1} u^{(n)}(s) ds, \ n-1 < q \leq n, \ \xi > 0,$$

where $n \in \mathbb{N}$ and the operator ${}^c\mathcal{D}^q$, satisfies the following properties:

$$\mathcal{I}_0^q {}^c\mathcal{D}^q u(\xi) = u(\xi) - \sum_{k=0}^{n-1} \frac{u^{(k)}(0)}{k!} \xi^k, \ \xi > 0, \tag{2.5}$$
$${}^c\mathcal{D}^q \mathcal{I}_0^q u(\xi) = u(\xi), \ n-1 < q \leq n.$$

2.2. **Shifted Jacobi polynomials.** Let $I = [-1, 1]$ and $\nu, \sigma > -1$. A sequence of polynomials $\{\mathcal{J}_n^{\nu,\sigma}(\xi)\}_{n=0}^\infty$ that fulfill the Sturm-Liouville equation [18, 39]

$$\partial_\xi \Big((1-\xi)^{\nu+1} (1+\xi)^{\sigma+1} \partial_\xi \mathcal{J}_n^{\nu,\sigma}(\xi) \Big) + \lambda_n^{\nu,\sigma} (1-\xi)^\nu (1+\xi)^\sigma \mathcal{J}_n^{\nu,\sigma}(\xi) = 0, \ \xi \in I, \ n = 0, 1, 2, \ldots,$$

with $\lambda_n^{\nu,\sigma} = n(n+\nu+\sigma+1)$, named as the Jacobi polynomials. The Jacobi polynomials $\mathcal{J}_n^{\nu,\sigma}(\xi)$ of degree n can be written in analytical form as:

$$\mathcal{J}_n^{\nu,\sigma}(\xi) = \frac{\Gamma(n+\nu+1)}{n!\Gamma(n+\nu+\sigma+1)} \sum_{k=0}^n \binom{n}{k} \frac{\Gamma(n+k+1+\nu+\sigma)}{\Gamma(k+1+\nu)} (\frac{\xi-1}{2})^k,$$

where $\mathcal{J}_0^{\nu,\sigma}(\xi) = 1$ and $\mathcal{J}_1^{\nu,\sigma}(\xi) = \frac{1}{2}(\nu+\sigma+2)\xi + \frac{1}{2}(\nu-\sigma)$.

The set of Jacobi polynomials with respect to weight function $\omega^{\nu,\sigma}(\xi) = (1-\xi)^\nu (1+\xi)^\sigma$, is a complete and orthogonal system in $L^2(I)$, i.e it has the property

$$\int_I \mathcal{J}_n^{\nu,\sigma}(\xi) \mathcal{J}_m^{\nu,\sigma}(\xi) \omega^{\nu,\sigma}(\xi) d\xi = h_n^{\nu,\sigma} \delta_{nm},$$

where

$$h_n^{\nu,\sigma} = \|\mathcal{J}_n^{\nu,\sigma}\|^2_{\omega^{\nu,\sigma}} = \frac{2^{\nu+\sigma+1}\Gamma(n+\nu+1)\Gamma(n+\sigma+1)}{(2n+\nu+\sigma+1)\Gamma(n+\nu+\sigma+1)n!},$$

and δ_{nm} is the Kronecker delta function. Now, let $\Lambda = [0, L]$ and $\overset{*}{\omega}{}^{\nu,\sigma}(\eta) = \omega^{\nu,\sigma}(\frac{2}{L}\xi - 1)$. By using the change of variable $\eta = \frac{2}{L}\xi - 1$, the analytic form of the shifted Jacobi polynomial is defined as:

$$\overset{*}{\mathcal{J}}{}_n^{\nu,\sigma}(\eta) = \sum_{k=0}^n \frac{(-1)^{n-k}\Gamma(n+\nu+1)\Gamma(n+k+\nu+\sigma+1)}{\Gamma(k+\nu+1)\Gamma(n+\nu+\sigma+1)(n-k)!k!L^k} \eta^k, \tag{2.6}$$

where $\overset{*}{\mathcal{J}}{}_n^{\nu,\sigma}(0) = (-1)^n \frac{\Gamma(n+\nu+1)}{\Gamma(\sigma+1)n!}$. Hence, the orthogonality condition is

$$\int_\Lambda \overset{*}{\mathcal{J}}{}_j^{\nu,\sigma}(\eta) \overset{*}{\mathcal{J}}{}_k^{\nu,\sigma}(\eta) \overset{*}{\omega}{}^{\nu,\sigma}(\eta) d\eta = \overset{*}{h}{}_j^{\nu,\sigma} \delta_{jk}, \tag{2.7}$$

where

$$\overset{*}{h}{}_j^{\nu,\sigma} = \frac{L^{\nu+\sigma+1}\Gamma(j+\nu+1)\Gamma(j+\sigma+1)}{(2j+\nu+\sigma+1)\Gamma(j+\nu+\sigma+1)\Gamma(j+1)}.$$

2.3. **Fractional Jacobi functions.** The fractional Jacobi functions $\mathcal{FJ}_n^{\lambda}(\tau)$ with $\lambda > 0$ and $\eta \in [0, L]$ are defined from the shifted Jacobi polynomials through the coordinate transform $\tau = \eta^{\lambda}$ as follows:

$$\mathcal{FJ}_n^{\lambda}(\tau) = \overset{*}{\mathcal{J}}{}_n^{\nu,\sigma}(\eta^{\lambda}).$$

Based on the relationship given in Equation (2.7), it can be easily verified that these functions are mutually orthogonal with respect to the weight function

$$\overset{*}{\omega}{}^{\nu,\sigma,\lambda}(\tau) = \lambda\tau^{\lambda(1+\sigma)-1}(L^{\lambda} - \tau^{\lambda})^{\nu},$$

i.e.,

$$\int_{\Lambda} \mathcal{FJ}_j^{\lambda}(\tau)\mathcal{FJ}_k^{\lambda}(\tau)\,\overset{*}{\omega}{}^{\nu,\sigma,\lambda}(\tau)d\tau = \overset{*}{h}{}_j^{\nu,\sigma,\lambda}\delta_{jk},\ j,k \geq 0,$$

where

$$\overset{*}{h}{}_j^{\nu,\sigma,\lambda} = \frac{L^{\lambda(\nu+\sigma+1)}\Gamma(j+\nu+1)\Gamma(j+\sigma+1)}{(2j+\nu+\sigma+1)\Gamma(j+\nu+\sigma+1)\Gamma(j+1)}.$$

Thus, for any $\mu \in L^2_{\overset{*}{\omega}{}^{\nu,\sigma,\lambda}}(\Lambda)$ we have

$$\mu(\tau) = \sum_{i=0}^{\infty} \mu_i \mathcal{FJ}_i^{\lambda}(\tau),$$

where the cofficients μ_i are given by

$$\mu_i = \frac{1}{\overset{*}{h}{}_i^{\nu,\sigma,\lambda}} \int_0^L \mu(\tau)\mathcal{FJ}_i^{\lambda}(\tau)\overset{*}{\omega}{}^{\nu,\sigma,\lambda}(\tau)d\tau,\ i = 0, 1, 2, \ldots. \tag{2.8}$$

In practical applications, the focus is typically on the first $(N+1)$ terms of the shifted Jacobi functions. Consequently, the function $\mu(\tau)$ can be represented in the following manner:

$$\mu_N(\tau) \simeq \sum_{i=0}^{N} \mu_i \mathcal{FJ}_i^{\lambda}(\tau) = \mathcal{B}^T \varrho(\tau),$$

where

$$\mathcal{B}^T = [\mu_0, \mu_1, \ldots, \mu_N],$$
$$\varrho(\tau) = [\mathcal{FJ}_0^{\lambda}(\tau), \mathcal{FJ}_1^{\lambda}(\tau), \ldots, \mathcal{FJ}_N^{\lambda}\}(\tau)]^T.$$

Let $\mathcal{FJ}_N^{\lambda}(\tau)$ denote the Jacobi functions defined on the interval I. For any function $\mu(\tau) \in C(\Lambda)$, the Jacobi-Gauss quadrature formulas can be expressed as:

$$\int_0^L \mu(\tau)\overset{*}{\omega}{}^{\nu,\sigma,\lambda}(\tau)d\tau \simeq \sum_{j=0}^{N} \overset{*}{\omega}{}_j^{\nu,\sigma,\lambda}\mu(\tau_j). \tag{2.9}$$

where

$$\tau_j = L(\frac{\xi_j + 1}{2})^{\frac{1}{\lambda}}, \qquad j = 0, 1, \cdots, N, \tag{2.10}$$

and $\{\xi_j\}_{j=0}^N$ are the roots of $\mathcal{J}_{N+1}^{\nu,\sigma}(\xi)$ and $\{\overset{*}{\omega}{}_j^{\nu,\sigma,\lambda}\}_{j=0}^N$ are the corresponding weights introduced in [8] defined as

$$\overset{*}{\omega}{}_j^{\nu,\sigma,\lambda} = (\frac{L^{\lambda}}{2})^{\nu+\sigma+1}\omega_j, \qquad j = 0, 1, \cdots, N,$$

where

$$\omega_j = \frac{\overset{\sim}{\nu}{}_N^{\nu,\sigma}}{(1-\xi_j^2)\Big(\partial_\xi \mathcal{J}_{N+1}^{\nu,\sigma}(\xi_j)\Big)^2} = \frac{\nu_N^{\nu,\sigma}}{\mathcal{J}_N^{\nu,\sigma}(\xi_j)\partial_\xi \mathcal{J}_{N+1}^{\nu,\sigma}(\xi_j)},\ j=0,1,\ldots,N, \tag{2.11}$$

and

$$\overset{\sim}{\nu}{}_N^{\nu,\sigma} = \frac{2^{\nu+\sigma+1}\Gamma(N+\nu+2)\Gamma(N+\sigma+2)}{(N+1)!\Gamma(N+\nu+\sigma+2)},$$
$$\nu_N^{\nu,\sigma} = \frac{2^{\nu,\sigma}(2N+\nu+\sigma+2)\Gamma(N+\nu+1)\Gamma(N+\sigma+1)}{(N+1)!\Gamma(N+\nu+\sigma+2)}.$$

In this section, we focus on computing the fractional integral of shifted Jacobi functions. A key aspect of the proposed methodology is establishing the derivative of fractional functions with respect to themselves. To formalize this relationship, we present the following theorem.

Theorem 2.3. *Let $\mathcal{F}\mathcal{J}_n^\lambda(\tau)$ be the shifted Jacobi functions Then we have*

$$\mathcal{I}_0^q \mathcal{F}\mathcal{J}_i^\lambda(\tau) = \sum_{j=0}^{N} \Delta(i,j)\mathcal{F}\mathcal{J}_j^\lambda(\tau),\ i=0,1,\ldots,N, \tag{2.12}$$

where

$$\Delta(i,j) = \sum_{k=0}^{i} \zeta_{ijk},$$

and

$$\zeta_{ijk} = \frac{(-1)^{i-k}\Gamma(i+\sigma+1)\Gamma(i+k+\nu+\sigma+1)\Gamma(k\lambda+1)}{\Gamma(k+\sigma+1)\Gamma(i+\nu+\sigma+1)\Gamma(k\lambda+q+1)(i-k)!k!} \times \sum_{h=0}^{j} \frac{(-1)^{j-h}\Gamma(j+h+\nu+\sigma+1)\Gamma(\nu+1)\Gamma(h+k+\frac{q}{\lambda}+\sigma+1)(2j+\nu+\sigma+1)j!}{\Gamma(j+\nu+1)\Gamma(h+\sigma+1)\Gamma(h+\frac{q}{\lambda}+k+\nu+\sigma+2)(j-h)!h!} L^q. \tag{2.13}$$

Proof. The shifted Jacobi functions $\mathcal{F}\mathcal{J}_n^\lambda(\tau)$ have an analytical form as described in (2.6). By utilizing the linear properties of fractional integration, we can combine Equations (2.1) and (2.3) to obtain the following result:

$$\mathcal{I}_0^q \mathcal{F}\mathcal{J}_j^\lambda(\tau) = \sum_{k=0}^{j} \frac{(-1)^{j-k}\Gamma(j+\sigma+1)\Gamma(j+k+\nu+\sigma+1)}{\Gamma(k+\sigma+1)\Gamma(j+\nu+\sigma+1)(j-k)!k!L^{\lambda k}}\mathcal{I}^q\tau^{\lambda k}$$
$$= \sum_{k=0}^{j} \frac{(-1)^{j-k}\Gamma(j+\sigma+1)\Gamma(j+k+\nu+\sigma+1)\Gamma(k\lambda+1)}{\Gamma(k+1+\sigma)\Gamma(j+\nu+\sigma+1)\Gamma(k+q+1)(j-k)!k!\Gamma(k\lambda+q+1)L^{\lambda k}}\tau^{\lambda k+q}. \tag{2.14}$$

By approximating $\tau^{\lambda k+q}$, using shifted fractional Jacobi functions, we derive the following results

$$\tau^{\lambda k+q} = \sum_{j=0}^{N} g_{kj}\mathcal{F}\mathcal{J}_j^\lambda(\tau), \tag{2.15}$$

where g_{kj} is given from (2.8) with $\mu(\tau)=\tau^{\lambda k+q}$, and this immediately gives

$$g_{kj}=\frac{(2j+\nu+\sigma+1)\Gamma(j+1)}{\Gamma(j+\nu+1)}L^{\lambda k+q}\times\sum_{h=0}^{j}\frac{(-1)^{j-h}\Gamma(j+h+\nu+\sigma+1)\Gamma(\nu+1)\Gamma(h+k+\sigma+\frac{q}{\lambda}+1)}{\Gamma(h+\sigma+1)\Gamma(h+\frac{q}{\lambda}+\nu+\sigma+k+2)(j-h)!h!},$$

$j=0,1,\ldots,N$. Using (2.14) and (2.15), we have

$$\mathcal{I}_0^q\mathcal{F}\mathcal{J}_i^{\lambda}(\tau)=\sum_{j=0}^{N}\Delta(i,j)\mathcal{F}\mathcal{J}_j^{\lambda}(\tau),\ i=0,1,\ldots,N, \tag{2.16}$$

where

$$\Delta(i,j)=\sum_{k=0}^{i}\zeta_{ijk}, \tag{2.17}$$

and

$$\zeta_{ijk}=\frac{(-1)^{i-k}\Gamma(i+\sigma+1)\Gamma(i+k+\nu+\sigma+1)\Gamma(k\lambda+1)}{\Gamma(k+\sigma+1)\Gamma(i+\nu+\sigma+1)\Gamma(k\lambda+q+1)(i-k)!k!}\times\sum_{h=0}^{j}\frac{(-1)^{j-h}\Gamma(j+h+\nu+\sigma+1)\Gamma(\nu+1)\Gamma(h+k+\frac{q}{\lambda}+\sigma+1)(2j+\nu+\sigma+1)j!}{\Gamma(j+\nu+1)\Gamma(h+\sigma+1)\Gamma(h+\frac{q}{\lambda}+k+\nu+\sigma+2)(j-h)!h!}L^q. \tag{2.18}$$

Hence, Equation (2.13) gives us the required result. □

3. Fractional Jacobi Function-Picard iteration method (FJF-PIM)

In this section, we propose a new method called FJF-PIM. This method provides a step-by-step process to solve fractional delay differential equations that have the following form:

$${}^c\mathcal{D}^q\mu(\tau)=f(\tau,\mu(\tau),\mu(\tau-r)),\ 0<\tau\le L,\ m-1<q\le m,\ m\in\mathbb{N}, \tag{3.1}$$

$$\mu(\tau)=\rho(\tau),\ \tau\in[-r,0],\ r>0, \tag{3.2}$$

$$\mu^{(l)}(0)=\mu_0^{(l)},\ l=0,1,\ldots,m-1, \tag{3.3}$$

where ${}^c\mathcal{D}^q\mu(\tau)$ denotes the well-known Caputo fractional derivative of order $q>0$. By performing fractional integration on both sides of Equation (3.1) and referring to (2.5), the fractional problem (3.1) with the initial conditions in (3.3) can be transformed into a fractional integral equation expressed as follows:

$$\mu(\tau)=\sum_{l=0}^{m-1}\frac{\tau^l\mu_0^{(l)}}{l!}+\frac{1}{\Gamma(q)}\int_0^{\tau}(\tau-s)^{q-1}f(s,\mu(s),\mu(s-r))ds, \tag{3.4}$$

$$\mu(\tau)=\rho(\tau),\ \tau\in[-r,0]. \tag{3.5}$$

According to (3.4), the Picard iteration process generates a sequence as follows:

$$\mu^i(\tau)=\sum_{l=0}^{m-1}\frac{\tau^l\mu_0^{(l)}}{l!}+\frac{1}{\Gamma(q)}\int_0^{\tau}(\tau-s)^{q-1}f(s,\mu^{i-1}(s),\mu^{i-1}(s-r))ds, \tag{3.6}$$

$$\mu^i(\tau)=\rho(\tau),\ \tau\in[-r,0], \tag{3.7}$$

where, $\mu^0(\tau)$ and $\mu^0(\tau-r)$ represent initial functions that satisfy the given initial conditions. Although Picard's method provides a straightforward iterative approach for solving Equation (3.1) using relation (3.6), its main drawback lies in the computational complexity of evaluating the fractional integral at each iteration. To address this challenge, we employ the FJF-PIM method.

The first step of FJF-PIM is to approximate the function $f(s,\mu^{i-1}(s),\mu^{i-1}(s-r))$ appearing on the right side of (3.6) by $\{\mathcal{FJ}_n^{\lambda}(s)\}_{n=0}^{N}$. Therefore,

$$f(s,\mu^{i-1}(s),\mu^{i-1}(s-r))\simeq\sum_{k=0}^{N}\tilde{f}_k^{i-1}\mathcal{FJ}_k^{\lambda}(s), \tag{3.8}$$

where the coefficients $\{\tilde{f}_k^{i-1}\}_{k=0}^{N}$ can be derived as

$$\tilde{f}_k^{i-1}=\frac{1}{h_k^{\nu,\sigma}}\sum_{j=0}^{N}f(s_j,\mu^{i-1}(s_j),\mu^{i-1}(s_j-r))\mathcal{FJ}_k^{\lambda}(s_j)\omega_j, \tag{3.9}$$

and

$$s_j=L(\frac{\tau_j+1}{2})^{\frac{1}{\lambda}},\ j=0,1,\cdots,N.$$

Substituting (3.8) in (3.6), for $\tau>r$ we have

$$\begin{aligned}\mu^i(\tau)=\sum_{l=0}^{m-1}\frac{\tau^l\mu_0^{(l)}}{l!}+\mathcal{I}^q(f(\tau,\mu^{i-1}(\tau),\mu^{i-1}(\tau-r)))&\simeq\sum_{l=0}^{m-1}\frac{\tau^l\mu_0^{(l)}}{l!}+\mathcal{I}^q\Big(\sum_{k=0}^{N}\tilde{f}_k^{i-1}\mathcal{FJ}_k^{\lambda}(\tau)\Big)\\&=\sum_{l=0}^{m-1}\frac{\tau^l\mu_0^{(l)}}{l!}+\sum_{k=0}^{N}\tilde{f}_k^{i-1}\mathcal{I}^q\Big(\mathcal{FJ}_k^{\lambda}(\tau)\Big).\end{aligned} \tag{3.10}$$

According to (2.15) and (2.16), we have

$$\begin{aligned}\mu^i(\tau)&\simeq\sum_{l=0}^{m-1}\frac{\mu_0^{(l)}}{l!}\sum_{j=0}^{N}C_{lj}\mathcal{FJ}_j^{\lambda}(\tau)+\sum_{k=0}^{N}\tilde{f}_k^{i-1}\sum_{j=0}^{N}\Delta(k,j)\mathcal{FJ}_j^{\lambda}(\tau)\\&=\sum_{j=0}^{N}\mathcal{FJ}_j^{\lambda}(\tau)\sum_{l=0}^{m-1}\frac{\mu_0^{(l)}}{l!}C_{lj}+\sum_{k=0}^{N}\tilde{f}_k^{i-1}\sum_{j=0}^{N}\Delta(k,j)\mathcal{FJ}_j^{\lambda}(\tau)\\&=\sum_{j=0}^{N}\mathcal{FJ}_j^{\lambda}(\tau)\Big(\sum_{l=0}^{m-1}\frac{\mu_0^{(l)}}{l!}C_{lj}+\sum_{k=0}^{N}\tilde{f}_k^{i-1}\Delta(k,j)\Big),\end{aligned} \tag{3.11}$$

where

$$\begin{aligned}C_{lj}=&\frac{(2j+\nu+\sigma+1)\Gamma(j+1)L^l}{\Gamma(j+\nu+1)}\\&\times\sum_{d=0}^{j}\frac{(-1)^{j-d}\Gamma(j+d+\nu+\sigma+1)\Gamma(\nu+1)\Gamma(d+l+\sigma+1)}{\Gamma(d+\sigma+1)\Gamma(d+l+\nu+\sigma+2)(j-d)!d!}.\end{aligned} \tag{3.12}$$

In the other hand, function $\mu^i(\tau)$ can be approximated as:

$$\mu^i(\tau)\simeq\sum_{j=0}^{N}a_j^i\mathcal{FJ}_j^{\lambda}(\tau). \tag{3.13}$$

Using (3.11) and (3.13), we obtain

$$\begin{aligned}&a_0^i\mathcal{FJ}_0^{\lambda}(\tau)+a_1^i\mathcal{FJ}_1^{\lambda}(\tau)+\cdots+a_N^i\mathcal{FJ}_N^{\lambda}(\tau)\simeq\\&\mathcal{FJ}_0^{\lambda}(\tau)\Big(\sum_{l=0}^{m-1}\frac{\mu_0^{(l)}}{l!}C_{l0}+\sum_{k=0}^{N}\tilde{f}_k^{i-1}\Delta(k,0)\Big)+\cdots+\mathcal{FJ}_N^{\lambda}(\tau)\Big(\sum_{l=0}^{m-1}\frac{\mu_0^{(l)}}{l!}C_{lN}+\sum_{k=0}^{N}\tilde{f}_k^{i-1}\Delta(k,N)\Big).\end{aligned} \tag{3.14}$$

The coefficients $\{a_j^i\}_{j=0}^{N}$ are determined by equating the corresponding coefficients of the shifted Jacobi functions on both sides of Equation (3.14). This process involves matching the terms associated with the same powers of the shifted

Jacobi functions, resulting in a system of equations. Solving this system yields the explicit values of the coefficients, given by:

$$a_j^i = \sum_{l=0}^{m-1} \frac{\mu_0^{(l)}}{l!} C_{lj} + \sum_{k=0}^{N} \tilde{f}_k^{i-1} \Delta(k,j), \;\; j = 0, 1, \dots N. \tag{3.15}$$

Without loss of generality, we can derive $\mu^i(\tau - r)$ from the initial function $\rho(\tau)$ and the approximated Jacobi series piecewise

$$\mu^i(\tau - r) \begin{cases} = \rho(\tau - r), & \tau \leq r, \\ \simeq \sum_{j=0}^{N} a_j^i \mathcal{F}\mathcal{J}_j^{\lambda}(\tau - r), & \tau > r. \end{cases} \tag{3.16}$$

4. Matrix-Vector form of the FJF-PIM

To improve the efficiency and computational performance of the FJF-PIM method, we propose a more concise matrix-vector representation. The approximate solution $\mu^i(\tau)$ is determined by computing the coefficients $\{a_j^i\}_{j=0}^N$ of the Jacobi function using Equation (3.13). To simplify the calculations, we represent the coefficients of the approximate solution $\mu^i(\tau)$ in vector form as follows:

$$\boldsymbol{a}^i = [a_0, a_1, \dots, a_N]^T. \tag{4.1}$$

We also look at the solution $\mu^i(\tau)$ at specific points called shifted Jacobi-Gauss nodes (see Equation (2.10)). We'll write these values as a vector.

$$\boldsymbol{u}^i = [\mu^i(\tau_0), \mu^i(\tau_1), \dots, \mu^i(\tau_N)]^T. \tag{4.2}$$

Substituting (3.13) in (4.2), the vector μ^i can be obtained as

$$\boldsymbol{u}^i = \mathbb{J}_{\boldsymbol{u}} \boldsymbol{a}^i, \tag{4.3}$$

where

$$\mathbb{J}_{\boldsymbol{u}} = \begin{pmatrix} \mathcal{F}\mathcal{J}_0^{\lambda}(\tau_0) & \mathcal{F}\mathcal{J}_1^{\lambda}(\tau_0) & \cdots & \mathcal{F}\mathcal{J}_N^{\lambda}(\tau_0) \\ \mathcal{F}\mathcal{J}_0^{\lambda}(\tau_1) & \mathcal{F}\mathcal{J}_1^{\lambda}(\tau_1) & \cdots & \mathcal{F}\mathcal{J}_N^{\lambda}(\tau_1) \\ \vdots & \vdots & \ddots & \vdots \\ \mathcal{F}\mathcal{J}_0^{\lambda}(\tau_N) & \mathcal{F}\mathcal{J}_1^{\lambda}(\tau_N) & \cdots & \mathcal{F}\mathcal{J}_N^{\lambda}(\tau_N) \end{pmatrix}, \tag{4.4}$$

is a constant matrix. The vector $\boldsymbol{a}^i$ can be recalculated in the new form using equation (3.15) as:

$$\boldsymbol{a}^i = \begin{pmatrix} a_0^i \\ a_1^i \\ \vdots \\ a_N^i \end{pmatrix} = \begin{pmatrix} \sum_{l=0}^{m-1} \frac{\mu_0^{(l)}}{l!} C_{l0} + \sum_{k=0}^{N} \tilde{f}_k^{i-1} \Delta(k,0) \\ \sum_{l=0}^{m-1} \frac{\mu_0^{(l)}}{l!} C_{l1} + \sum_{k=0}^{N} \tilde{f}_k^{i-1} \Delta(k,1) \\ \vdots \\ \sum_{l=0}^{m-1} \frac{\mu_0^{(l)}}{l!} C_{lN} + \sum_{k=0}^{N} \tilde{f}_k^{i-1} \Delta(k,N) \end{pmatrix} \tag{4.5}$$

$$= \boldsymbol{U}_0 + \begin{pmatrix} \tilde{f}_0^{i-1}\Delta(0,0) + \tilde{f}_1^{i-1}\Delta(1,0) + \cdots + \tilde{f}_N^{i-1}\Delta(N,0) \\ \tilde{f}_0^{i-1}\Delta(0,1) + \tilde{f}_1^{i-1}\Delta(1,1) + \cdots + \tilde{f}_N^{i-1}\Delta(N,1) \\ \vdots \\ \tilde{f}_0^{i-1}\Delta(0,N) + \tilde{f}_1^{i-1}\Delta(1,N) + \cdots + \tilde{f}_N^{i-1}\Delta(N,N) \end{pmatrix}$$

$$= \boldsymbol{U}_0 + \begin{pmatrix} \Delta(0,0) & \Delta(1,0) & \cdots & \Delta(N,0) \\ \Delta(0,1) & \Delta(1,1) & \cdots & \Delta(N,1) \\ \vdots & & & \\ \Delta(0,N) & \Delta(1,N) & \cdots & \Delta(N,N) \end{pmatrix} \begin{pmatrix} \tilde{f}_0^{i-1} \\ \tilde{f}_1^{i-1} \\ \vdots \\ \tilde{f}_N^{i-1} \end{pmatrix} = \boldsymbol{U}_0 + \boldsymbol{M}\boldsymbol{f}^{\boldsymbol{i-1}}, \tag{4.6}$$

where

$$M = \begin{pmatrix} \Delta(0,0) & \Delta(1,0) & \cdots & \Delta(N,0) \\ \Delta(0,1) & \Delta(1,1) & \cdots & \Delta(N,1) \\ \vdots & & & \\ \Delta(0,N) & \Delta(1,N) & \cdots & \Delta(N,N) \end{pmatrix}, \tag{4.7}$$

$$\boldsymbol{U}_0 = \left(\sum_{l=0}^{m-1} \frac{\mu_0^l}{l!} C_{l0}, \quad \sum_{l=0}^{m-1} \frac{\mu_0^l}{l!} C_{l1}, \quad \ldots, \quad \sum_{l=0}^{m-1} \frac{\mu_0^l}{l!} C_{lN} \right)^T, \tag{4.8}$$

and

$$\boldsymbol{f}^{\boldsymbol{i-1}} = \left(\tilde{f}_0^{i-1}, \quad \tilde{f}_1^{i-1}, \quad \ldots, \quad \tilde{f}_N^{i-1} \right)^T, \tag{4.9}$$

Here, , $\boldsymbol{U}_0$ is a fixed vector, and $\boldsymbol{M}$ is a constant matrix. By substituting (3.9) into (4.9), we obtain the following:

$$\boldsymbol{f}^{\boldsymbol{i-1}} = \begin{pmatrix} \tilde{f}_0^{i-1} \\ \tilde{f}_1^{i-1} \\ \vdots \\ \tilde{f}_N^{i-1} \end{pmatrix} = \begin{pmatrix} \frac{1}{h_0^{\nu,\sigma}} \Big(f(\tau_0, \mu^{i-1}(\tau_0), \mu^{i-1}(\tau_0 - r)) \mathcal{F}\mathcal{J}_0^{\lambda}(\tau_0)\omega_0 \Big) \\ \frac{1}{h_1^{\nu,\sigma}} \Big(f(\tau_0, \mu^{i-1}(\tau_0), \mu^{i-1}(\tau_0 - r)) \mathcal{F}\mathcal{J}_1^{\lambda}(\tau_0)\omega_0 \Big) \\ \vdots \\ \frac{1}{h_N^{\nu,\sigma}} \Big(f(\tau_0, \mu^{i-1}(\tau_0), \mu^{i-1}(\tau_0 - r)) \mathcal{F}\mathcal{J}_N^{\lambda}(\tau_0)\omega_0 \Big) \end{pmatrix}$$

$$+ \cdots + \begin{pmatrix} \frac{1}{h_0^{\nu,\sigma}} \Big(f(\tau_N, \mu^{i-1}(\tau_N), \mu^{i-1}(\tau_N - r)) \mathcal{F}\mathcal{J}_0^{\lambda}(\tau_N)\omega_N \Big) \\ \frac{1}{h_1^{\nu,\sigma}} \Big(f(\tau_N, \mu^{i-1}(\tau_N), \mu^{i-1}(\tau_N - r)) \mathcal{F}\mathcal{J}_1^{\lambda}(\tau_N)\omega_N \Big) \\ \vdots \\ \frac{1}{h_N^{\nu,\sigma}} \Big(f(\tau_N, \mu^{i-1}(\tau_N), \mu^{i-1}(\tau_N - r)) \mathcal{F}\mathcal{J}_N^{\lambda}(\tau_N)\omega_N \Big) \end{pmatrix}$$

$$= \boldsymbol{H}\mathbb{J}_u^T \boldsymbol{W}\boldsymbol{F}^{\boldsymbol{i-1}}, \tag{4.10}$$

where

$$\boldsymbol{W} = diag\left(\omega_0, \omega_1, \ldots, \omega_N\right)_{N+1}, \tag{4.11}$$

$$\boldsymbol{H} = diag\left(\tfrac{1}{h_0^{\nu,\sigma}}, \tfrac{1}{h_1^{\nu,\sigma}}, \ldots, \tfrac{1}{h_N^{\nu,\sigma}} \right)_{N+1}, \tag{4.12}$$

$$\boldsymbol{F}^{\boldsymbol{i-1}} = \left(f(\tau_0, \mu^{i-1}(\tau_0), \mu^{i-1}(\tau_0 - r)), \ldots, f(\tau_N, \mu^{i-1}(\tau_N), \mu^{i-1}(\tau_N - r)) \right)^T. \tag{4.13}$$

Thus, from (4.5) and (4.10), one can get

$$\boldsymbol{a}^i = \boldsymbol{U}_0 + \boldsymbol{M}\boldsymbol{f}^{i-1} = \boldsymbol{U}_0 + \boldsymbol{M}\boldsymbol{H}\mathbb{J}_u^T \boldsymbol{W}\boldsymbol{F}^{\boldsymbol{i-1}} = \boldsymbol{U}_0 + \mathbb{J}_a \boldsymbol{F}^{\boldsymbol{i-1}}, \tag{4.14}$$

where $\mathbb{J}_a = \boldsymbol{MH}\mathbb{J}_u^T\boldsymbol{W}$ is a constant matrix.

Next, we analyze the behavior of $\mu^i(\tau - r)$ using a specialized series representation known as the Jacobi series in the subsequent step of the process. By applying Equation (2.10) to the condition $\tau_j - r \leq 0$, we obtain:

$$\xi_j \leq 2\sqrt[\lambda]{\frac{\tau_j}{L}} - 1.$$

Let $\hat{j}$ be the largest positive integer satisfying the inequality mentioned above. Equation (3.16) can then be discretized.

$$\mu^i(\tau_j - r)\begin{cases} = \rho(\tau_j - r), & j \leq \hat{j}, \\ \simeq \sum_{j=0}^{N} a_j^i \mathcal{FJ}_j^\lambda(\tau_j - r), & j > \hat{j}. \end{cases} \tag{4.15}$$

Take $\tau' = \tau - r$, such that $\mathcal{FJ}_n^\lambda(\tau - r) = \mathcal{FJ}_n^\lambda(\tau')$ for $n = 0, 1, , N$, we have

$$\boldsymbol{u}_r^i = [\mu^i(\tau_0'), \mu^i(\tau_1'), \ldots, \mu^i(\tau_N')]^T. \tag{4.16}$$

Substituting (4.15) in (4.16), the vector $\boldsymbol{u}_r^i$ can be obtained as

$$\boldsymbol{u}_r^i = \boldsymbol{\rho}_{\hat{j}} + \mathbb{J}_{\boldsymbol{r}}\boldsymbol{a}^i, \tag{4.17}$$

where

$$\mathbb{J}_{\boldsymbol{r}} = \begin{pmatrix} 0 & 0 & \cdots & 0 \\ \vdots & \vdots & \ddots & \vdots \\ 0 & 0 & \cdots & 0 \\ \mathcal{FJ}_0^\lambda(\tau_{\hat{j}+1}') & \mathcal{FJ}_1^\lambda(\tau_{\hat{j}+1}') & \cdots & \mathcal{FJ}_N^\lambda(\tau_{\hat{j}+1}') \\ \vdots & \vdots & \ddots & \vdots \\ \mathcal{FJ}_0^\lambda(\tau_N') & \mathcal{FJ}_1^\lambda(\tau_N') & \cdots & \mathcal{FJ}_N^\lambda(\tau_N') \end{pmatrix}, \tag{4.18}$$

and

$$\boldsymbol{\rho}_{\hat{j}} = [\rho(\tau_0 - r), \rho(\tau_1 - r), \ldots, \rho(\tau_{\hat{j}} - r), 0, \ldots, 0]^T. \tag{4.19}$$

Finally, the $(i+1)$-th Picard's iteration can be done by updating the values of μ^i and μ_r^i. We keep doing this until a specific condition

$$\|\mu^i - \mu^{i-1}\| = \max_{\tau \in [0,L]} |\mu^i(\tau) - \mu^{i-1}(\tau)| < \epsilon,$$

called the stopping criterion, is true.

5. Error analysis of the FJF-PIM

The convergence analysis of the FJF-PIM method is fundamental to verifying its reliability and accuracy. In this study, we conduct a rigorous analysis to establish the method's convergence in solving functional differential delay equations (FDDEs). This analysis provides a thorough examination of the convergence properties, ensuring that the numerical solutions systematically approach the exact solutions of the FDDEs. We identify sufficient conditions under which the FJF-PIM method converges and demonstrate that, under specific criteria imposed on the FDDEs, the iterative process leads to the exact solution. Considering the FDDE (3.1), the convergence criterion for the FJF-PIM method applied to the linear FDDE (3.1) is formally stated in the following theorem:

Theorem 5.1. *Suppose in system FDDE (3.1) the function f satisfied in the Lipschitz condition with respect to the second variable, i.e*

$$|f(\tau, \mu(\tau), \mu_r(\tau)) - f(\tau, \mu_1(\tau), \mu_{1r}(\tau))| < K_1\|\mu - \mu_1\| + K_2\|\mu_r - \mu_{1r}\|,$$

where K_1 and K_2 are the Lipschitz condition. The FJF-PIM method is convergent if and only if

$$\|\mathbb{J}_{\boldsymbol{u}}\|\|\mathbb{J}_a\|\Big(K_1 I + K_2\|\mathbb{J}_{\boldsymbol{r}}\|\|\mathbb{J}_u^{-1}\|\Big) < 1.$$

Proof. As we define in (4.3), we can write

$$\begin{aligned}\boldsymbol{u}^i - \boldsymbol{u}^{i-1} &= \mathbb{J}_{\boldsymbol{u}}\boldsymbol{a}^i - \mathbb{J}_{\boldsymbol{u}}\boldsymbol{a}^{i-1}\\ &= \mathbb{J}_{\boldsymbol{u}}(\boldsymbol{U}_0 + \mathbb{J}_a\boldsymbol{F}^{\boldsymbol{i-1}} - \boldsymbol{U}_0 - \mathbb{J}_a\boldsymbol{F}^{\boldsymbol{i-2}})\\ &= \mathbb{J}_{\boldsymbol{u}}\mathbb{J}_a(\boldsymbol{F}^{\boldsymbol{i-1}} - \boldsymbol{F}^{\boldsymbol{i-2}}).\end{aligned}$$

Therefore,

$$\begin{aligned}\|\boldsymbol{u}^i - \boldsymbol{u}^{i-1}\| &= \|\mathbb{J}_{\boldsymbol{u}}\mathbb{J}_a(\boldsymbol{F}^{\boldsymbol{i-1}} - \boldsymbol{F}^{\boldsymbol{i-2}})\|\\ &\le \|\mathbb{J}_{\boldsymbol{u}}\|\|\mathbb{J}_a\| \max_{0\le j\le N}|f(\tau_j,\mu^{i-1}(\tau_j),\mu_r^{i-1}(\tau_j)) - f(\tau_j,\mu^{i-2}(\tau_j),\mu_r^{i-2}(\tau_j))|.\end{aligned}$$

Using (4.2), (4.16),(4.17), $\boldsymbol{a}^i = \mathbb{J}_{\boldsymbol{u}}^{-\mathbf{1}}\boldsymbol{u}^i$, and also $\boldsymbol{u}_r^i = \boldsymbol{\rho}_{\tilde{j}} + \mathbb{J}_{\boldsymbol{r}}\mathbb{J}_{\boldsymbol{u}}^{-\mathbf{1}}\boldsymbol{u}^i$ we obtain

$$\begin{aligned}\|\boldsymbol{u}^i - \boldsymbol{u}^{i-1}\| &\le \|\mathbb{J}_{\boldsymbol{u}}\|\|\mathbb{J}_a\|\Big(K_1\|\boldsymbol{u}^{i-1} - \boldsymbol{u}^{i-2}\| + K_2\|\boldsymbol{u}_r^{i-1} - \boldsymbol{u}_r^{i-2}\|\Big)\\ &\le \|\mathbb{J}_{\boldsymbol{u}}\|\|\mathbb{J}_a\|\Big(K_1\|\boldsymbol{u}^{i-1} - \boldsymbol{u}^{i-2}\| + K_2\|\mathbb{J}_{\boldsymbol{r}}\mathbb{J}_{\boldsymbol{u}}^{-\mathbf{1}}(\boldsymbol{u}^{i-1} - \boldsymbol{u}^{i-2})\|\Big)\\ &\le \|\mathbb{J}_{\boldsymbol{u}}\|\|\mathbb{J}_a\|\Big(K_1 I + K_2\|\mathbb{J}_{\boldsymbol{r}}\|\|\mathbb{J}_{\boldsymbol{u}}^{-\mathbf{1}}\|\Big)\|\boldsymbol{u}^{i-1} - \boldsymbol{u}^{i-2}\|\\ &\vdots\\ &\le \Big(\|\mathbb{J}_{\boldsymbol{u}}\|\|\mathbb{J}_a\|\Big(K_1 I + K_2\|\mathbb{J}_{\boldsymbol{r}}\|\|\mathbb{J}_{\boldsymbol{u}}^{-\mathbf{1}}\|\Big)\Big)^{i-1}\|\boldsymbol{u}^1 - \boldsymbol{u}^0\|,\end{aligned}$$

where I is an $(N+1)$ identity matrix. Thus, we will have

$$\|\boldsymbol{u}^i - \boldsymbol{u}^{i-1}\| \le \Big(\|\mathbb{J}_{\boldsymbol{u}}\|\|\mathbb{J}_a\|\Big(K_1 I + K_2\|\mathbb{J}_{\boldsymbol{r}}\|\|\mathbb{J}_{\boldsymbol{u}}^{-\mathbf{1}}\|\Big)\Big)^{i-1}\|\boldsymbol{u}^1 - \boldsymbol{u}^0\|.$$

Hence, it is clear that if $\|\mathbb{J}_{\boldsymbol{u}}\|\|\mathbb{J}_a\|\Big(K_1 I + K_2\|\mathbb{J}_{\boldsymbol{r}}\|\|\mathbb{J}_{\boldsymbol{u}}^{-\mathbf{1}}\|\Big) < 1$ we will obtain

$$\lim_{i\to\infty}\|\boldsymbol{u}^i - \boldsymbol{u}^{i-1}\| = 0,$$

which completes the proof. □

Remark 5.2. The initial value problem (3.1) has a unique global solution under the hypothesis that the function f is continuous and satisfies a Lipschitz condition ith respect to the second variable (see Theorem 3.1 in [10])

6. Numerical Examples

In this section, we present several examples to illustrate the high accuracy and effectiveness of the FJF-PIM approach. By comparing our results with those obtained using other methods, we demonstrate the accuracy and efficiency of the FJF-PIM.

To begin, we determine the order of convergence (CO) for the FJF-PIM, following the findings reported in [2]:

$$CO = \frac{\log(\frac{errorN_1}{errorN_2})}{\log(\frac{N_2}{N_1})},$$

where $errorN_1$ denotes the error associated with the approximation of degree N_1. The maximum absolute errors for $u(x)$ are represented by L_∞, while the maximum absolute errors for the differences between two successive iterations are denoted by E_l. For comparison, we define the following measure:

$$L_\infty = \|u_{Ex}(x) - u_{App}(x)\|_\infty,$$

TABLE 1. The maximum of the absolute error of the Present method with $q = 3$, $\lambda = 1$, $N = 10$ and $\nu = \sigma = 0$ for Example 6.1.

τ	Present method	GWM
0.1	$7.8406e-17$	$2.02e-12$
0.3	$4.5511e-17$	$8.48e-10$
0.5	$1.0568e-16$	$5.26e-17$
0.7	$4.7481e-17$	$9.89e-12$
0.9	$7.6671e-17$	$3.03e-08$
1	$4.5901e-16$	$3.78e-07$

TABLE 2. Maximum of the absolute error of $\mu(\tau)$, for $q = 3$, $\nu = \sigma = 0$ with the convergence order for Example 6.1.

N	L_∞	CO
5	$3.3636e-08$	-
10	$4.5901e-16$	26.1269
15	$7.2513e-25$	49.9821

where $u_{Ex}(x)$ and $u_{App}(x)$ represent the exact and approximate solutions, respectively.

All computations were performed on a laptop with the following specifications: an Intel Core $i5$-6198DU CPU, 8 GB of RAM, a base clock speed of 2.30 GHz, and a maximum clock speed of 2.40 GHz. The system operates on a 64-bit architecture. The computational tasks were carried out using Maple 2020, which significantly facilitated the analysis and implementation of complex numerical computations.

Example 6.1. Consider the pantograph differential equation of third order [3, 12, 14, 38]

$$
\begin{aligned}
&{}^{c}\mathcal{D}^{q}\mu(\tau) = -\mu(\tau) - \mu(\tau - 0.3) + \exp(-\tau + 0.3),\ 2 < q \leq 3,\\
&u(0) = 1,\ \mu'(0) = -1,\ \mu''(0) = 1,\ 0 \leq \tau \leq 1.
\end{aligned}
$$

The exact solution, when $q = 3$ is $\mu(\tau) = \exp(-\tau)$.

Since this example does not have an exact solution for non-integer values of q, the efficiency of the proposed method is assessed by evaluating the maximum error between two consecutive iterations. This approach effectively demonstrates the performance of the method for different values of q in this specific example.

The computational results of this example are displayed in Table 1 and Figure 1. In Table 1, we compare the results of the proposed method for $\lambda = 1$, $\nu = \sigma = 0$, and $q = 3$ with those obtained using the novel collocation method based on the Genocchi wavelet (GWM) presented in [12]. Figure 2, shows the approximate and exact solutions for different values of q. Table 1 clearly demonstrates that the proposed method achieves high accuracy when compared to the other methods referenced. In Table 2, we investigate the order of convergence (CO) of the new algorithm for various values of N. Additionally, Table 3 shows the maximum error between two consecutive iterations for this particular example.

The example was numerically solved using the Haar wavelet collocation technique (HWCT), as outlined in [3], with a maximum error of 2.9790×10^{-8}. Furthermore, the results presented in Table 1 highlight that the method proposed in this study exhibits greater efficiency than the approach discussed in [3].

Example 6.2. We consider the following FDDE [23, 38]

$$
\begin{aligned}
&{}^{c}\mathcal{D}^{q}\mu(\tau) = \mu(\tau - r) - \mu(\tau) + \frac{2}{\Gamma(3-q)}\tau^{2-q} - \frac{1}{\Gamma(2-q)}\tau^{1-q} + 2r\tau - r^2 - r,\ 0 \leq \tau \leq 1,\\
&\mu(\tau) = 0,\ \tau \leq 0,\ 0 < q \leq 1.
\end{aligned}
$$

The exact solution is $\mu(\tau) = \tau^2 - \tau$. In Table 4, we compare the results of the proposed method with the Fractional-order Fibonacci-Hybrid Functions Method (FFHFM) from [38] for the case where $\lambda = q = 0.5$ and $\nu = \sigma = 0$. The

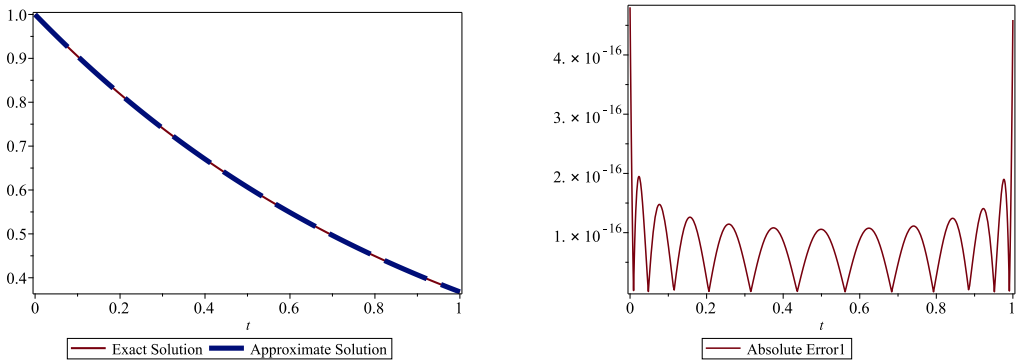

FIGURE 1. The exact and approximate solutions (left) and absolute error of solution by proposed method (right) in Example 6.1.

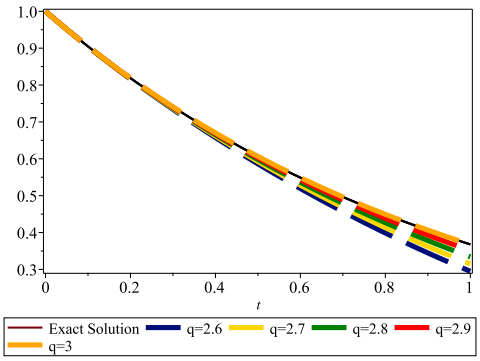

FIGURE 2. The approximate and exact solutions for different choices of q in Example 6.1.

TABLE 3. Maximum of the absolute error of $\mu(\tau)$, for $\nu = \sigma = 0$ and different choices of q with the convergence order for Example 6.1.

q	L_∞
2.7	$5.5047e-27$
2.8	$3.2509e-28$
0.9	$5.2605e-26$

data in Table 4 demonstrate that the proposed method is both efficient and accurate for solving this problem. The numerical results show that the solutions obtained with this approach converge to the analytical solution. Additionally, we solved this problem for $q = 0.5$ and $\lambda = 1$, and the results in Table 6 further confirm the effectiveness of our method in addressing this specific problem. Figure 3 provides a comparative analysis of the exact and approximate responses for various values of the parameter q. The figure also displays the absolute error associated with the proposed method, specifically for the case where $q = \lambda = 0.5$ and $\nu = \sigma = 0$. The graph in Figure 3 demonstrates a close match between the approximate and exact solutions, underscoring the effectiveness of our approach. Furthermore, we conducted a comprehensive error analysis, allowing for a more detailed evaluation of the method's accuracy and efficiency. The data in Tables 4 and 6 reveal that, for a fractional order of $q = 0.5$, the optimal value of λ is also 0.5. Table 7 presents the maximum absolute error achieved by our method for various combinations of the parameters a and b. Finally, in Table 5, we examine the order of convergence (CO) of the proposed algorithm for different values of N.

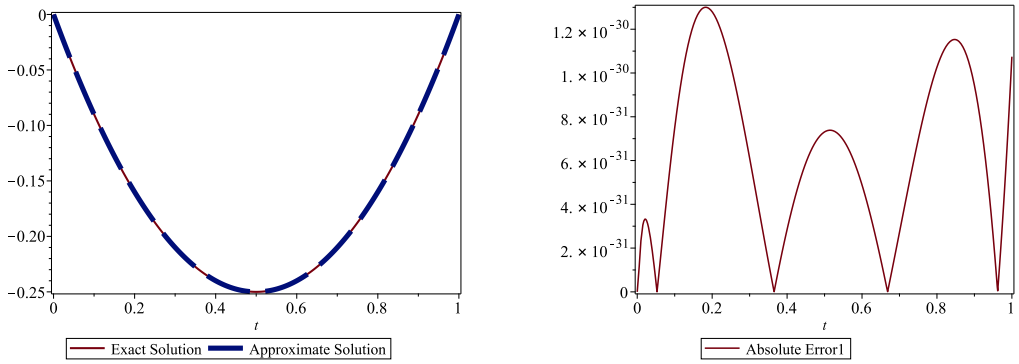

FIGURE 3. The exact and approximate solutions (left) and absolute error of solution by proposed method (right) for $q = \lambda = 0.5$, $\nu = \sigma = 0$ and $N = 5$ in Example 6.2.

TABLE 4. Comparison of maximum of the absolute error of the Present method with $q = \lambda = 0.5$, $N = 5$, $r = 0.1$ and $\nu = \sigma = 0$ with FFHFM [38] for Example 6.2.

τ	Present method	FFHFs [38]
0.1	$7.4926e-31$	$1.58642e-15$
0.3	$6.1126e-31$	$7.84349e-06$
0.5	$7.3089e-31$	$4.44156e-06$
0.7	$2.7221e-31$	$1.24645e-05$
0.9	$9.4348e-31$	$3.43936e-05$

TABLE 5. Maximum of the absolute error of $\mu(\tau)$, for $q = \lambda = 0.5$, $\nu = \sigma = 0$ with the convergence order for Example 6.2.

N	L_∞	CO
5	$1.2e-30$	-
10	$1.0e-30$	0.2630
15	$6.0e-31$	1.2599
20	$7.0e-31$	0.5358

TABLE 6. Comparison of maximum of the absolute error of the Present method with $q = 0.5$, $\lambda = 1$, $N = 5$, $r = 0.1$ and $\nu = \sigma = 0$ with FFHFM [38] for Example 6.2.

τ	Present method	FFHFs[38]
0.1	$3.46850e-04$	$3.37404e-04$
0.3	$7.74502e-04$	$1.50058e-04$
0.5	$1.91622e-04$	$1.37223e-03$
0.7	$3.60773e-04$	$1.09563e-02$
0.9	$2.02441e-04$	$9.51393e-03$

TABLE 7. Maximum of the absolute error of $\mu(\tau)$, for $q = \lambda = 0.5$ and different choices of ν, σ for Example 6.3.

	$\nu = -\sigma = 0.5$	$\nu = \sigma = 0.5$	$\nu = -\sigma = -0.5$	$\nu = \sigma = -0.75$	$\nu = \sigma = -0.99$
L_∞	$3.01235e-30$	$1.74513e-30$	$7.145228e-31$	$3.68672e-31$	$4.71279e-31$

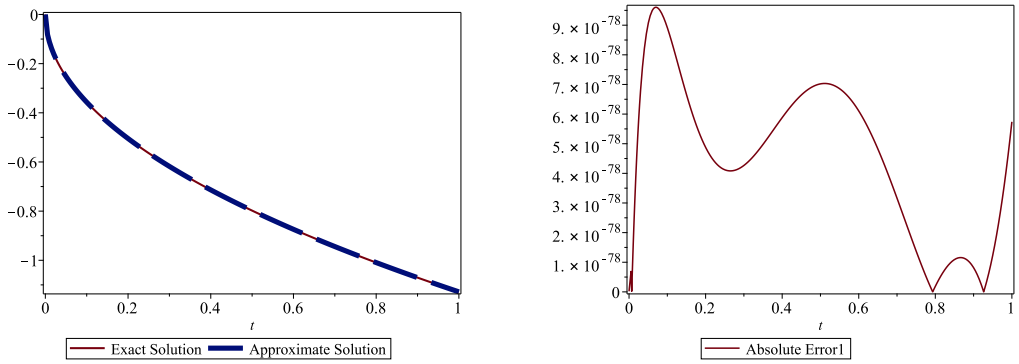

FIGURE 4. The exact and approximate solutions (left) and absolute error of solution by proposed method (right) for $q = \lambda = 0.5$, $\nu = \sigma = 0$ and $N = 5$ in Example 6.3.

TABLE 8. Comparison of maximum of the absolute error of the Present method with $q = \lambda = 0.5$, $N = 3$ and $\nu = \sigma = 0$ with HWCT method ($N = 2048$) for Example 6.3.

	Present method	HWCT[3]
L_∞	$4.0e-79$	$3.78360e-03$

TABLE 9. Maximum of the absolute error of $\mu(\tau)$, for $q = 0.5$, $\nu = \sigma = 0$ and different choices of λ for Example 6.3.

	$\lambda = 1$	$\lambda = 0.7$	$\lambda = 0.6$	$\lambda = 0.5$	$\lambda = 0.3$
L_∞	$1.4e-02$	$3.0e-02$	$1.2e-02$	$4.0e-79$	$2.0e-03$

Example 6.3. We consider the following FDDE [3]

$$
\begin{aligned}
&{}^c\mathcal{D}^q\mu(\tau) = \mu(\tau - r) - \tau,\ 0 \le \tau \le 1,\ 0 < q \le 1,\ r = 1,\\
&\mu(\tau) = \tau,\ -1 \le \tau < 0.
\end{aligned}
$$

The exact solution for $q = 0.5$ is $\mu(\tau) = -\frac{2\sqrt{\tau}}{\Gamma(\frac{1}{2})}$.

The graph in Figure 4 demonstrates the close correspondence between the approximate solution and the exact solution, which highlights the effectiveness of our approach. Furthermore, we have performed a more in-depth analysis by investigating the error, allowing for a more detailed assessment of the accuracy and efficiency of the method. In Table 8, we compare the results of the present method with HWCT method [3] for the case of $\lambda = q = 0.5$ and $\nu = \sigma = 0$. In Table 9, the maximum of the absolute error of $\mu(\tau)$ is presented, for the case where $q = 0.5$, $\nu = \sigma = 0$, and different values of the parameter λ.

Example 6.4. Consider the following fractional delay differential equation [23]

$$
\begin{aligned}
&{}^c\mathcal{D}^q\mu(\tau) = \frac{\Gamma(2.5)}{\Gamma(2.5-q)}\tau^{\frac{3}{2}-q} + \mu^2(\tau - r) - \mu(\tau) - (\tau - r)^3 + \tau^{\frac{3}{2}},\ 0 \le \tau \le 1,\\
&\mu(\tau) = 0,\ -r \le \tau \le 0,\ 0 < q \le 1,\ r = 1.
\end{aligned}
$$

The exact solution is $\mu(\tau) = \tau^{\frac{3}{2}}$. The system of equations was solved numerically when the parameters $r = 0.1$, $q = 0.75$, $\lambda = 0.6$. The absolute and relative errors were then calculated and presented in Table 10. In this research, the example presented has been solved using the proposed method, and the results have been compared with those obtained from methods fractional Adams method (FAM), new predictor-corrector method (NPCM) and family of predictor-corrector methods based on fractional backward difference formulae termed as FBD-PCM [23].

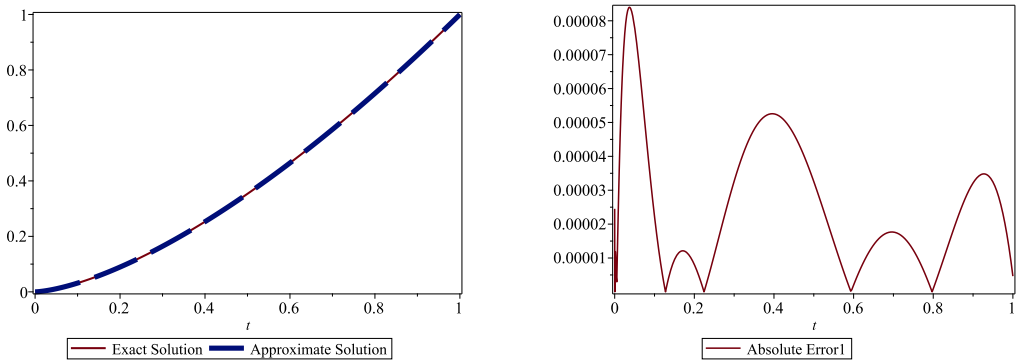

FIGURE 5. The exact and approximate solutions (left) and absolute error of solution by proposed method (right) for $q = 0.75$, $\lambda = 0.6$, $\nu = \sigma = 0$ and $N = 5$ in Example 6.4.

TABLE 10. Comparison of maximum of the absolute error of the present method with $q = 0.75$, $\lambda = 0.6$, $N = 5$ and $\nu = \sigma = 0$ with the methods presented in [23] for Example 6.4.

τ	Present method	FAM[23]	NPCM [23]	FBD-PCM2 [23]
0.2	$8.07166e-06$	$2.1968e-05$	$2.1005e-05$	$1.9429e-05$
0.4	$5.25333e-05$	$1.5571e-05$	$1.4326e-05$	$1.0606e-05$
0.6	$2.01232e-06$	$1.3550e-05$	$1.2037e-05$	$5.4097e-06$
0.8	$9.16439e-07$	$1.3538e-05$	$1.1662e-05$	$9.7216e-07$
1.0	$4.64327e-06$	$1.5224e-05$	$1.2789e-05$	$3.9765e-06$

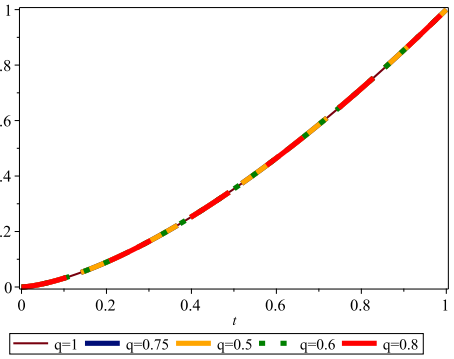

FIGURE 6. The approximate and exact solutions for different choices of q in Example 6.4.

The results indicate that our proposed method demonstrates superior efficiency. The graph in Figure 5 illustrates the close alignment between the approximate solution and the exact solution, which underscores the effectiveness of our approach. Figure 6, shows the approximate and exact solutions for different choices of q.

Example 6.5. The Hutchinson model is a mathematical model that describes the rate of population growth. according to this model, the rate of population growth at any given time is dependent on specific relationships and factors that are unique to that particular time period. The Hutchinson model can be expressed through an equation that captures

TABLE 11. maximum absolute error for difference between two consecutive iterations of the Present method with $q = \lambda = 0.5$, $N = 5$, $l = 11$ and different choices of ν, σ for Example 6.5.

	$\nu = \sigma = 0$	$\nu = \sigma = 0.5$	$a = -b = 0.5$	$\nu = \sigma = -0.75$	$\nu = \sigma = -0.99$
E_l	$8.3134e-29$	$7.6239e-29$	$1.0264e-28$	$1.1560e-28$	$1.1464-28$

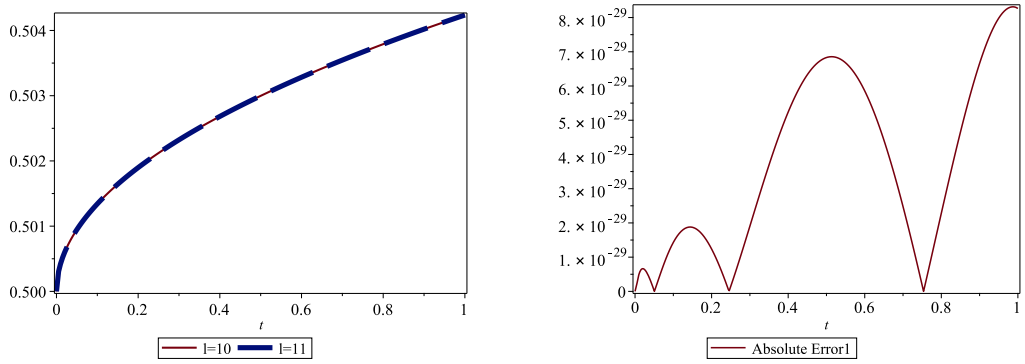

FIGURE 7. The exact and approximate solutions (left) and absolute error of solution by proposed method (right) for $q = \lambda = 0.5$, $\nu = \sigma = 0$ and $N = 5$ in Example 6.5.

these dynamic relationships and their influence on the population growth rate and its equation is as follows.

$$
\begin{aligned}
&{}^{c}\mathcal{D}^{q}\mu(\tau) = e\mu(\tau) - \frac{e}{d}\,\mu(\tau)\,\mu(\tau - r),\ 0 \le \tau \le 1,\ 0 < q \le 1,\\
&\mu(\tau) = 0.5,\ -r \le \tau \le 0.
\end{aligned}
$$

The analytical solution to the equation representing the Hutchinson model is not available, as indicated by the reference [38]. Given this limitation, the primary goal is to ensure the convergence of the proposed method for solving or modeling the population growth dynamics described by the Hutchinson model. For this approach, consider the error norm as follows

$$E_l = \max_{\tau \in [0,L]} |\mu^{l}(\tau) - \mu^{l-1}(\tau)|.$$

The graph in Figure 7 illustrates the close alignment between the approximate solution and the exact solution, which underscores the effectiveness of our approach. The calculated maximum absolute error for difference between two consecutive iterations in Table 11 for $r = 0.2$, $e = 0.015$ and $d = 1$.

Example 6.6. Consider the nonlinear delay FODE [3]

$$
\begin{aligned}
&{}^{c}\mathcal{D}^{q}\mu(\tau) = \mu(\tau - \frac{1}{2}) + \mu^{3}(\tau) + \frac{2}{\Gamma(1.5)}\tau^{0.5} - (\tau - 0.5)^{2} - \tau^{6},\ 0 \le \tau \le 1,\\
&\mu(\tau) = \tau^{2}\ \ -r \le \tau \le 0,\ 1 < q \le 2,
\end{aligned}
$$

with the initial conditions $\mu(0) = 0$ and $\mu'(0) = 0$. The exact solution, when $q = 1.5$ is $\mu(\tau) = \tau^2$.

The graph in Figure 8 illustrates the strong agreement between the approximate and exact solutions, highlighting the effectiveness of our proposed approach.

In Table 12, we compare the results of the present method for the case $q = 1.5$, $\lambda = 0.5$, and $\nu = \sigma = 0$ with those obtained using the Haar Wavelet Collocation Technique (HWCT) [3]. The data presented in Table 12 demonstrates that the proposed method provides an accurate and efficient solution for this specific problem.

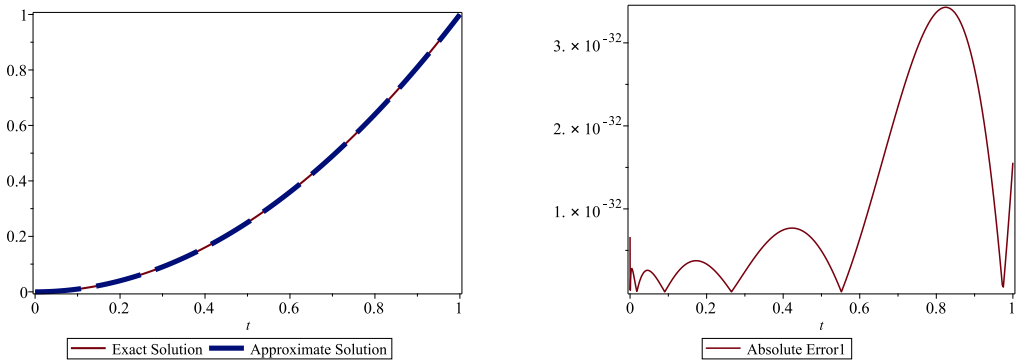

FIGURE 8. The exact and approximate solutions (left) and absolute error of solution by proposed method (right) for $q = 1.5$, $\lambda = 0.5$, $\nu = \sigma = 0$ and $N = 5$ in Example 6.6.

TABLE 12. Comparison of maximum of the absolute error of the Present method with $q = 1.5$, $\lambda = 0.5$, $N = 5$ and $\nu = \sigma = 0$ with HWCT method ($N = 256$) for Example 6.6.

	Present method	HWCT[3]
L_∞	$3.0e-32$	$2.2571e-02$

7. Conclusion

In this study, we introduced the fractional Jacobi function-Picard iteration method (FJF-PIM) as an efficient numerical approach for solving nonlinear fractional delay differential equations (FDDEs). This method provides a computational framework that effectively addresses the complexities of FDDEs while ensuring accurate numerical solutions.

To enhance computational efficiency, we also developed a matrix-vector formulation of the FJF-PIM. The proposed method was compared against existing numerical techniques and exact solutions, demonstrating superior accuracy and efficiency. Additionally, a convergence analysis was conducted to validate the reliability and stability of the approach.

The FJF-PIM has proven to be a highly effective method for solving nonlinear FDDEs, offering notable advantages such as high accuracy and computational efficiency. To further assess its practical applicability, we applied the method to several applicable problems, including the Pantograph and Hutchinson equations. The results confirmed that FJF-PIM outperforms other numerical methods in terms of accuracy and convergence.

This study contributes significantly to the field of fractional calculus by introducing a powerful and versatile numerical technique for solving FDDEs. The demonstrated reliability and efficiency of FJF-PIM make it a valuable tool for researchers and practitioners in this domain. The findings of this work are expected to facilitate further advancements and applications of fractional calculus in various scientific and engineering disciplines.

Author declaration

The authors have no conflicts to disclose.

References

[1] M. H. Akrami, A. Poya, and M. A. Zirak, *Solving the general form of the fractional Black–Scholes with two assets through reconstruction variational iteration method,* Results Appl. Math, *22* (2024), 100444.

[2] M. M. Alsuyuti, E. H. Doha, S. S. Ezz-Eldien, B. I. Bayoumi, and D. Baleanu, *Modified Galerkin algorithm for solving multitype fractional differential equations,* Math. Methods Appl. Sci., *42*(5) (2019), 1389–1412.

[3] R. Amin, K. Shah, M. Asif, and I. Khan, *A computational algorithm for the numerical solution of fractional order delay differential equations,* Appl. Math. Comput., *402* (2021), 125863.

[4] S. Ansari and M. H. Akrami, *An effective approach for solving nonlinear fractional initial value problems: The fractional Legendre-Picard iteration method,* J. Math. Ext., *18*(3) (2024), 1–29.
[5] S. Ansari and M. H. Akrami, *Fractional Jacobi–Picard iteration method using Gauss–Seidel technique for solving a system of nonlinear fractional differential equations,* Alex. Eng. J., *108* (2024), 261–272.
[6] S. Ansari and M. H. Akrami, *Fractional Bernoulli-Picard iteration: A powerful tool for solving time-fractional partial differential equations,* Fract. Calc. Appl. Anal., *28* (2025), 2036–2055.
[7] D. Baleanu, R. L. Magin, S. Bhalekar, and V. Daftardar-Gejji, *Chaos in the fractional order nonlinear Bloch equation with delay.* Commun. Nonlinear Sci. Numer. Simul., *25*(1-3) (2015), 41–49.
[8] A. Bhrawy and M. Zaky, *A fractional-order Jacobi Tau method for a class of time-fractional PDEs with variable coefficients,* Math. Methods Appl. Sci., *39*(7) (2016), 1765–1779.
[9] Z. Chen and Q. Gou, *Piecewise Picard iteration method for solving nonlinear fractional differential equation with proportional delays,* Appl. Math. Comput., *348* (2019), 465–478.
[10] N. Cong and H. Tuan, *Existence, uniqueness, and exponential boundedness of global solutions to delay fractional differential equations,* Mediterr. J. Math., *14* (2017), 1–12.
[11] K. L. Cooke, *Differential—difference equations,* International symposium on nonlinear differential equations and nonlinear mechanics, Elsevier, 1963, 155–171.
[12] H. Dehestani, Y. Ordokhani, and M. Razzaghi, *A numerical technique for solving various kinds of fractional partial differential equations via Genocchi hybrid functions,* Rev. Real Acad. Cienc. Exactas Fis. Nat. - A: Mat., *113* (2019), 3297–3321.
[13] H. Dehestani, Y. Ordokhani, and M. Razzaghi, *On the applicability of Genocchi wavelet method for different kinds of fractional-order differential equations with delay,* Numer. Linear Algebra Appl., *26*(5) (2019), e2259.
[14] H. Dehestani, Y. Ordokhani, and M. Razzaghi, *Numerical technique for solving fractional generalized pantograph-delay differential equations by using fractional-order hybrid bessel functions,* Int. J. Appl. Comput. Math., *6* (2020), 1–27.
[15] M. S. Hadi, M. Lakestani, and B. Nemati Saray, *The wavelet Galerkin method for fractional delay differential equations,* Calcolo, *62*(48) (2025).
[16] J. K. Hale, *Functional differential equations,* Analytic Theory of Differential Equations: The Proceedings of the Conference at Western Michigan University, Kalamazoo, from 30 April to 2 May 1970, Springer, 2006, 9–22.
[17] M. Heydari and M. Razzaghi, *A highly accurate method for multi-term time fractional diffusion equation in two dimensions with ψ-Caputo fractional derivative,* Results Appl. Math., *23* (2024) 100481.
[18] M. Heydari and M. Razzaghi, *Jacobi polynomials method for a coupled system of Hadamard fractional Klein–Gordon–Schrödinger equations,* Alex. Eng. J., *107* (2024) 73–86.
[19] S. Karami, M. Heydari, D. Baleanu, and M. Bayram, *Modified hat functions for constrained fractional optimal control problems with ψ-Caputo derivative*, Commun. Nonlinear Sci. Numer. Simul., *143* (2025), 108657.
[20] M. Kazemi, R. Rahul, and A. Yaghoobnia, *Applications of measure of noncompactness for solvability of Hadamard fractional integral equations*, Comput. Appl. Math., *44*(1) (2025), 1–14.
[21] N. A. Khan, M. Ali, A. Ara, M. I. Khan, S. Abdullaeva, and M. Waqas, *Optimizing Pantograph fractional differential equations: A Haar wavelet operational matrix method*, Partial Differ. Equ. Appl. Math., (2024), 100774.
[22] H. R. Khodabandelo, E. Shivanian, and S. Abbasbandy, *A novel shifted Jacobi operational matrix method for nonlinear multi-terms delay differential equations of fractional variable-order with periodic and anti-periodic conditions*, Math. Methods Appl. Sci., *45*(16) (2022), 10116–10135.
[23] M. Kumar, A. Jhinga, and V. Daftardar-Gejji, *Higher order numerical methods for fractional delay differential equations*, Indian J. Pure Appl. Math., (2024), 1–22.
[24] M. Lakestani and R. Tuntas, *Efficient solution for multi-delay fractional optimal control problems via cubic B-Splines*, Optim. Control Appl. Methods, *46*(6) (2025), 2411–2422.
[25] C. Li and F. Zeng, *Numerical methods for fractional calculus*, 24. CRC Press, 2015.
[26] B. P. Moghaddam, S. Yaghoobi, and J. Tenreiro Machado, *An extended predictor–corrector algorithm for variable-order fractional delay differential equations*, J. Comput. Nonlinear Dyn., *11*(6) (2016).

[27] R. Mohammadzadeh and M. Lakestani, *Optimal control of linear time-delay systems by a hybrid of block-pulse functions and biorthogonal cubic hermite spline multiwavelets*, Optim. Control Appl. Methods, *39* (2018), 357–376.
[28] A. D. Myshkis, *General theory of differential equations with retarded arguments*, Usp. Mat. Nauk, *4*(5) (1949), 99–141.
[29] S. B. Norkin et al, *Introduction to the theory and application of differential equations with deviating arguments*, Academic Press, 1973.
[30] Z. Odibat and D. Baleanu, *Numerical simulation of nonlinear fractional delay differential equations with Mittag-Leffler kernels,* Appl. Numer. Math., *201* (2024), 550–560.
[31] I. Podlubny, *Fractional differential equations: an introduction to fractional derivatives, fractional differential equations, to methods of their solution and some of their applications*. Mathematics in science and engineering. Academic Press, London, 1999.
[32] S. Qureshi, *Real life application of Caputo fractional derivative for measles epidemiological autonomous dynamical system*, Chaos, Solitons & Fractals, *134* (2020), 109744.
[33] P. Rahimkhani and M. H. Heydari, *Numerical investigation of ψ-fractional differential equations using wavelets neural networks*, Comput. Appl. Math., *44*(1) (2025), 54.
[34] P. Rahimkhani, Y. Ordokhani, and E. Babolian, *A new operational matrix based on Bernoulli wavelets for solving fractional delay differential equations,* Numer. Algorithms, *74* (2017), 223–245.
[35] H. Rasekhinezhad, S. Abbasbandy, T. Allahviranloo, and E. Babolian, *A reproducing kernel method for solving nonlocal functional differential equations with delayed or advanced arguments*, Comput. Methods Differ. Equ., *14*(1) (2026), 1–13.
[36] A. M. Regal and D. Kumar S, *Fitted mesh cubic spline tension method for singularly perturbed delay differential equations with integral boundary condition*, Comput. Methods Differ. Equ., *13*(2) (2025), 618–633.
[37] S. Sabermahani, Y. Ordokhani, and S.-A. Yousefi, *Fibonacci wavelets and their applications for solving two classes of time-varying delay problems*, Optim. Control Appl. Methods, *41*(2) (2020), 395–416.
[38] S. Sabermahani, Y. Ordokhani, and S.-A. Yousefi, *Fractional-order Fibonacci-hybrid functions approach for solving fractional delay differential equations*, Eng. Comput., *36* (2020), 795–806.
[39] J. Shen, T. Tang, and L.-L. Wang, *Spectral methods: algorithms, analysis and applications*, Springer Science & Business Media, *41*, 2011.
[40] R. Sipahi and S. I. Niculescu, *Deterministic time-delayed traffic flow models: A survey*, Complex time-delay systems: theory and applications, 2010, 297–322.
[41] M. Tafakkori-Bafghi, G. Barid Loghmani, M. Heydari, and X. Bai, *Jacobi-Picard iteration method for the numerical solution of nonlinear initial value problems*, Math. Methods Appl. Sci., *43*(3) (2020), 1084–1111.
[42] M. Usman, M. Hamid, M. S. U. Khalid, R. U. Haq, and M. Liu, *A robust scheme based on novel-operational matrices for some classes of time-fractional nonlinear problems arising in mechanics and mathematical physics*, Numer. Methods Partial Differ. Equ., *36*(6) (2020), 1566–1600.
[43] F. Zakipour and A. Saadatmandi, *A new Bernoulli–Picard iteration method for nonlinear initial value problems*, Vietnam J. Math., (2024), 1–20.
[44] T. Zhang, X. Meng, and T. Zhang, *SVEIRS: a new epidemic disease model with time delays and impulsive effects*, Abstr. Appl. Anal., 2014, Wiley Online Library, 2014, 542154.
[45] J. Zhao, X. Jiang, and Y. Xu, *Generalized Adams method for solving fractional delay differential equations*, Math. Comput. Simul., *180* (2021), 401–419.
[46] Q. Zhou, Y. Wang, L. Ma, and Y. Liu, *Piecewise Jacobi–Gauss spectral collocation simulations for a multi-particle model involving processing delay*, Comput. Appl. Math., *43*(6) (2024), 1–24.